Electrochimica Acta 53 (2008) 6568–6574

Contents lists available at ScienceDirect

Electrochimica Acta

journal homepage: www.elsevier.com/locate/electacta

Rapid impedance scanning QCM for electrochemical applications based on miniaturized hardware and high-performance curve fitting

F. Wudy, M. Multerer, C. Stock, G. Schmeer, H.J. Gores*

Institut für Physikalische und Theoretische Chemie der Universität Regensburg, Universita"tsstrasse 31, D-93053 Regensburg, Germany

ARTICLE INFO

Article history:
Received 20 March 2008
Received in revised form 24 April 2008
Accepted 28 April 2008
Available online 4 May 2008

Keywords:
Impedance
Quarz microbalance
Linear data fit algorithm
Copper electrodeposition and dissolution
Electropolymerization of aniline

ABSTRACT

An impedance system for QCM measurements is described which produces a much higher information content than existing oscillator methods. The new system is favourably priced, and fits on a small single printed circuit board. The use of a personal computer with a dedicated software algorithm enables fast fitting of the collected data and allows high flexibility without the need of a change in hardware. It was shown that this QCM device is able to collect stable and high-quality data with the – in electrochemistry not very commonly used – small and very inexpensive 0.55 in. diameter quartz devices, even under heavy load. A full spectrum containing serial and parallel resonance frequencies, with a band width of 20 kHz can be scanned within 200 ms at a resolution of 0.2 Hz. Lowering requirements, e.g. by scanning series resonance frequency only, the acquisition time can be reduced drastically. The electrochemical applications (EQCM) so developed was checked using known electrochemical tasks such as copper deposition, dissolution and the electropolymerization of aniline.

1. Introduction

Oscillating quartz crystals have been used for a long time, not only as a frequency determining part in electronic applications, but also as a mass sensitive sensors implicated by Sauerbrey [1]. A special way to cut the synthetically grown quartz crystal, the so-called AT-cut [2,3] in shear-vibrational mode [4] is commonly used due to its temperature stability and its mechanical oscillation behaviour performing a thickness shear deformation. Acting as mass sensitive devices and having the potential to determine mass changes down to the nanogram scale, quartz crystals have been utilized in a number of research fields, such as monitors for deposition and gas analyzers [5], electrochemical applications (EQCM) [6], biological investigations [7] and studies of physical properties of liquids, such as viscosity or density of fluids [8,9] and gases [10]. The electronic behaviour of such quartz crystal sensors can be understood in terms of the Butterworth van-Dyke (BVD) equivalent circuit [2,3] and its variations [11,12].

An impedance scan is shown in Fig. 1. The differences in the frequency response of the quartz crystal depending on its load, here air or water, can easily be recognized. Series and parallel resonance frequencies (ν_s and ν_p) are located at the minimum and maximum of the magnitude curve, respectively. The phase shift changes its sign from capacitive to inductive and back to capacitive at these two frequencies. At high levels of damping the dynamic range decreases dramatically, a change of sign does not occur any more. However, this change of sign in phase is needed by most of the common oscillator circuitries [13], used to determine one of the resonance frequencies of such a quartz sensor, either (ν_s or ν_p), according to the design. Furthermore, the quality factor [3,14] of the quartz decreases directly with the extent of loading, leading to a divergence of ν_s and ν_p Due to spurious phase shifts induced by the circuitry of the oscillator design, exact oscillation at one of these two frequencies is rendered impossible. Usually, the oscillator works at an operation point somewhere in between. The expanding gap between ν_s and ν_p and the reduced slope in frequency and phase changes entail a large increase in the error of frequency determination. Complex circuits with adjustments subject to the actual system, whose parameters can change during measurement, are necessary to overcome these problems [15]. So it can happen that the oscillator ceases to work in a correct manner during measurement. Finally, the frequency of the oscillation has to be determined. This necessitates the implementation of a frequency counter [16]. Simple digital counters can be used. To maximize the resolution to measurement time ratio, reciprocal counters [17] with a very high primary clock or downmixing designs can be implemented, increasing the complexity. To obtain a resolution of seven digits, a measuring time of several hundred ms is sufficient [18].

Another approach gathering information on the behaviour of the quartz, not only at the resonance frequency but covering the entire impedance spectrum, has been shown by a group from the Otto-von-Guericke University (Magdeburg, Germany) [13,18–20].

* Corresponding author.
E-mail address: heiner.gores@eqcm.de (H.J. Gores).

0013-4686/$ – see front matter © 2008 Elsevier Ltd. All rights reserved.
doi:10.1016/j.electacta.2008.04.079

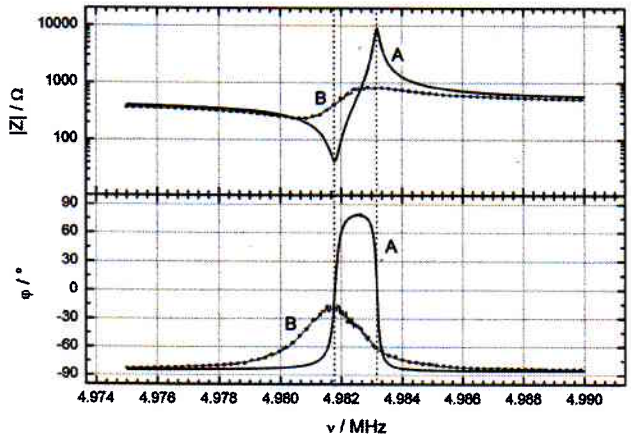

Fig. 1. A typical impedance scan is shown for a quartz crystal in air (A), and being damped with water (B), measured using a Solartron SI 1260 impedance analyzer.

They have built up a precision network analyzer focussed on frequencies typically applied in QCM research. Delia and Vanysek [21] show how to use an impedance analyzer from Solartron, specifically for electrochemical applications.

These systems all have in common, that they are quite complex and that the obtained spectrum has to be fitted via the BVD Equation to find the desired parameters. Therefore, such devices are very slow in data collection with about one data point per second [15] which prevents fast in-situ measurements. In fitting data to the BVD model afterwards, the non-linear Levenberg-Marquardt [21] or simplex algorithms find common use. However, very good start parameters are required and the fit is very sensitive to the frequency range used. Furthermore, it is quite slow even on fast computers because of the large number of parameters needed. Failures in convergence of fits often occur.

The approach described here strikes a balance between complexity [22] and information density. Inspired by Bruschi et al. [23], circuitry was built that allows results to be obtained very quickly, and employs low-cost hardware that is also affordable for industrial use.

2. Experimental

2.1. Electronic setup

Our goal was to develop a simple, functional and cost-effective hardware platform, performing most of the acquisition tasks in software. A resulting advantage is that modifications, e.g. a change in controlling and evaluation algorithms, can be very easily implemented, since there is no need to change the hardware setup.

As shown in Fig. 2, a single chip programmable logic device (PLD) from Lattice Semiconductor acts as the core of the QCM. The PLD connects to a free programmable synthesizer chip (DDS) to drive the frequency sweeps. The synthesizer delivers a sine wave at the output. Simple circuitry (DAC) adjusts the amplitude of the output signal within 0.05–8.33 V_{rms} in 4096 steps. Both, the PLD and the DDS are provided with the same primary 80 MHz clock (CLK). To filter out feedthrough from clock and digital lines, a dedicated 4th order low-pass filter (LP) with a cut-off frequency of 10 or 15 MHz is connected on the load side. Subsequently, the sine wave, variable in frequency (from 1 to 10 or 15 MHz) and amplitude, is amplified by a high-speed and powerful current-feedback operational amplifier. Using a medium-impedance AC-coupling network (AC cpl.), the signal is injected into the quartz crystal. This arrangement allows use of the circuitry within an electrochemical setup,

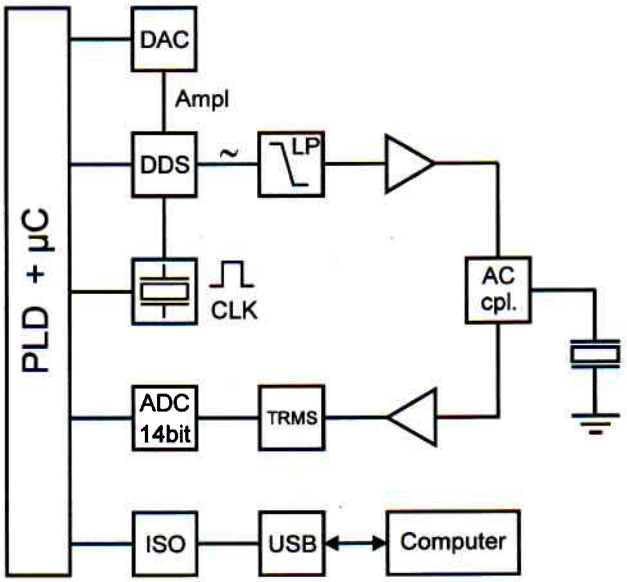

Fig. 2. Electronic setup for the fast impedance scanning QCM, for details see text.

with one quartz crystal electrode acting as the working electrode. The signal is afterwards coupled out by this network. Using a precise single chip RMS-to-DC (TRMS) converter, linear over the whole frequency range, in combination with a low-pass filter the logarithm of the quartz impedance response is evaluated by a 14-bit successive approximation A/D-converter (ADC). The PLD collects the data, forms the arithmetic mean at every frequency step over at least two measurements and delivers the data to a USB host controller that sends the data to a personal computer. A bus isolator (ISO) avoids ground-loops. An additional microcontroller (µC) performs the high-level tasks, such as calculating start- and stop-frequencies, the sweep rate including the frequency step width, and controls the PLD. The primary clock (CLK) working at 80 MHz allows a resolution of about 20 mHz in frequency. The highest achievable frequency sweep rate is about 500,000 measurement events per second. Therefore, assuming typical parameters for a loaded quartz crystal, a full spectrum containing serial and parallel resonance frequencies, with a band width of 20 kHz can be scanned within 200 ms at a resolution of 0.2 Hz. Lowering requirements, e.g. by scanning series resonance frequencies only, and/or a decrease in frequency resolution, the acquisition time can be reduced drastically.

2.2. Software setup

A run-time optimized program written in C collects the data from the USB bus, and performs data integrity checks. The spectrum is displayed immediately. After an overview scan, the user has the possibility to refine the resolution and start- and stop- frequencies in a very comfortable manner, so that the ROI (region of interest) can be measured with high resolution. In choosing the ROI the user is not limited to the fundamental oscillation. The ROI can be set to every harmonic very easily. When using an array of crystals with different resonance frequencies each crystal is accessible by setting the ROI to its resonance frequency. To determine the series and the parallel resonance frequencies, the spectrum is fitted on the Padé approximant [24,25]

$$y = \frac{p(\nu)}{1 + Q(\nu)} = \frac{A + B\nu + C\nu^2}{1 + D\nu + E\nu^2 + F\nu^3}. \quad (1)$$

This Equation can be linearized to

$$y = p(\nu) - Q(\nu)y, \quad (2)$$

enabling a fast linear least-squares fit to determine the coefficients of the function in Eq. (1).

After the optimization, the minimum (ν_s) and maximum (ν_p) locations of the fit function are identified. Together with χ^2, a reduced quality factor [23], $\hat{Q} = \nu_p/\nu_s$ is calculated during this process enabling users to detect errors quickly. All data, including fit parameters, are stored making error detection during a long-term measurement possible. A fuzzy-logic software algorithm controls a smooth frequency setpoint tracing for the automated operating mode. A direct software interlink to the controlling software for the cyclic voltammetry (CV) experiment makes it possible to get direct data in the format: voltage–current–frequency, with a minimal uncertainty in time ensuring the highest possible digital resolution.

2.3. Chemical systems

Experiments were undertaken using a standard three-electrode arrangement housed in a glass cell containing the quartz carrier made from KEL-F in the bottom of the cell. All electrochemical potentials reported are given with respect to the saturated Ag/AgCl electrode RE-5B from BAS. The top side of a 6 MHz gold-coated 0.55 in. quartz crystal SC-101 from Maxtek (CA, USA) with an electrode area of 0.357 cm^2 represents the working electrode in contact with the liquid. A platinum ring was used as counter electrode. The CV experiments were conducted with a self-built precision potentiostat with a direct digital link to the QCM forming the EQCM equipment. The quartz surface was cleaned after each measurement using 0.1 M H_2SO_4 performing several anodic CV scans in the range 0.35–0.7 V until no more changes in the cyclic voltammogram could be recognized. Copper deposition experiments were realized using an aqueous electrolyte solution consisting of 200 g H_2O, 20.4 g H_2SO_4 and 4.993 g $CuSO_4 \cdot 5H_2O$. Solutions were prepared using Millipore quality water and p.a. chemicals. 30.00 g of the electrolyte were transferred into the measurement cell. Oxygen was removed from solution by passing purified nitrogen for 20 min. Series of experiments were performed by standard additions of solid KCl p.a. to the electrolyte. Voltammograms and frequency shift evolution curves were recorded according to the Cl^- concentrations given in moles per kg solution (molonity [26]).

To show the behaviour of the EQCM under heavy loads, a viscoelastic polymer film from polymerized aniline (PANI) was created on the working electrode of the quartz crystal according to literature [27,28]. Aniline was used freshly distilled under inert gas at a concentration of 0.1 mol/L in 1 mol/L phosphoric acid. A cyclic voltammetry experiment was performed for the electropolymerization within −0.24 and 0.9 V, applying a sweep rate of 10 mV/s. This experiment was monitored over 25 cycles with the QCM.

3. Results and discussion

Fig. 3 shows a typical cyclic voltammogram and a frequency shift evolution curve for an experiment with the copper electrolyte without chloride. The scan starts at a potential of 0.75 V and sweeps cathodically (V = 10 mV/s) to −0.12 V. As long as cathodic voltages are applied to the cell the frequency decreases showing copper plating onto the working electrode. Scanning in the anodic direction from −0.12 V the electrode mass still increases up to about 0.07 V. Here the maximum mass of the electrode is reached. Sweeping further in the anodic direction an anodic current and an increase in the frequency of the quartz crystal shows copper dissolution. The surface profile of the quartz crystal was investigated by atomic force microscopy (AFM) in non-contact mode. No significant changes, especially in the roughness of the surface could be found before and after the electrodeposition. Typical structured copper crystallites with diameters of 0.5 to 5 μm are found on the yet rough surface.

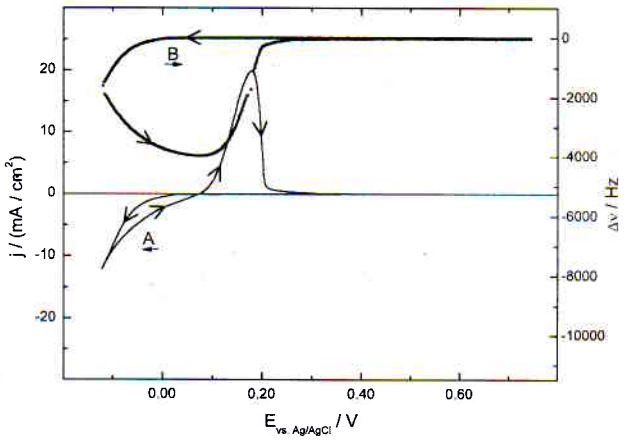

Fig. 3. Cyclic voltammogram (A) and frequency–potential diagram (B) of 0.1 M $CuSO_4 \cdot 5H_2O$ + 1 M H_2SO_4. No KCl was added. V = 10 mV/s.

Plotting the frequency shift $\Delta\nu$ versus the variation of charge ΔQ [29] as shown in Fig. 4 results in a linear dependency for this system. The slopes of 80.8 kHz/C for the cathodic part of the measurement and 81.3 kHz/C for the anodic part of the measurement are in good agreement yielding a maximum error of 0.35%. The arithmetic mean of 81.1 kHz/C corresponds to a calibration parameter C_f of 246 Hz/μg with respect to copper. An examination of Sauerbrey's expression for the calibration parameter [1]

$$C_f = \frac{2f_{ro}^2}{A\sqrt{\rho_Q G_Q}} \quad (3)$$

which depends only on the intrinsic properties of the quartz (A is the surface, ρ_Q the density, and G_Q the shear modulus of the quartz and f_{ro} is the resonance frequency of the total resonator) yields a C_f parameter of 228 Hz/μg. This agreement is satisfactory given in the many assumptions made in the rather simple Sauerbrey model.

In Figs. 5 and 6, the same system with a Cl^- concentration of 4.22×10^{-4} mol/kg is shown. The range of the potential was chosen in such a manner that dissolution of gold in the presence of Cl^-

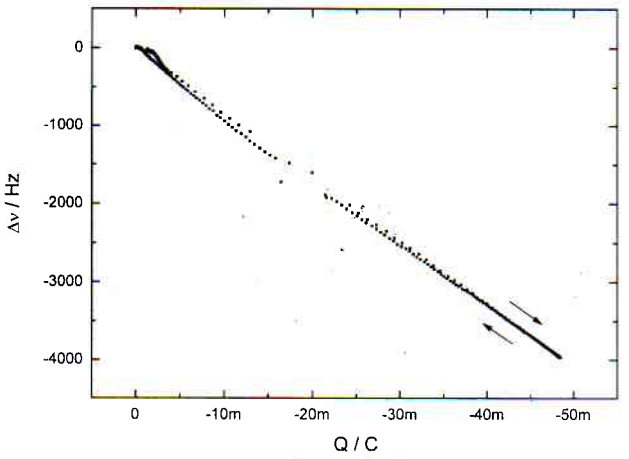

Fig. 4. Calibration measurement. Change of resonance frequency as function of charge Q. A slope of 81.1 kHz/C was determined. This equals 246 Hz/μg copper.

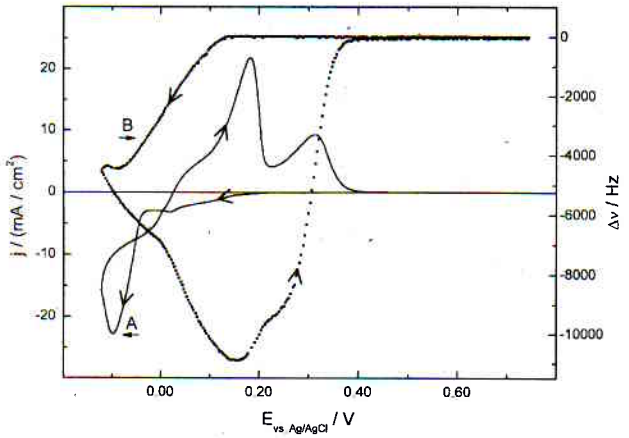

Fig. 5. Cyclic voltammogram (A) and frequency shift curve (B) of 0.1 M $CuSO_4 \cdot 5H_2O$ + 1 M H_2SO_4 with added KCl. $m(Cl^-)$ = 42.2 mmol/kg. V = 10 mV/s.

could not occur as is sometimes reported in the literature [30]. The preservation of the gold electrode can also be seen in Fig. 5 where no hysteresis in frequency is observed at the starting potential of the scans.

In contrast to the chloride-free system two anodic partially overlapping peaks are recorded. The electrode mass not only increases during the cathodic part of the scan but also during the first anodic peak. Dissolution of copper is superimposed on the anodic generation of solid CuCl on the electrode, as recently reported by Kologo et al. [31]. During the second anodic peak the CuCl(s) is oxidized to Cu^{2+} and Cl^-. The resonance frequency returns to its initial value showing a completely reversible system. This behaviour holds true for chloride concentrations far higher than those investigated by Kologo et al. Fig. 7 shows the influence of the chloride concentration on voltammograms and frequency–potential diagrams. Comparing the chloride free system A with the systems B–E containing increasing amounts of chloride the occurrence of a second superimposed peak in the frequency–potential diagram is obvious. Also the maximum frequency shift is no longer achieved during cathodic deposition of copper but during the first anodic peak of the current. The current density of systems B–E shows a second anodic peak, which is not existing in system A. This peak can be attributed to the dissolution of CuCl(s) [31–33].

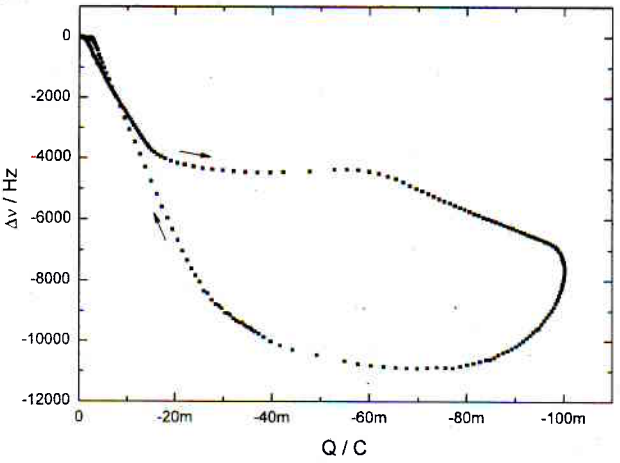

Fig. 6. Change of resonance frequency as function of charge Q of 0.1 M $CuSO_4 \cdot 5H_2O$ + 1 M H_2SO_4 with added KCl. $m(Cl^-)$ = 42.2 mmol/kg. V = 10 mV/s.

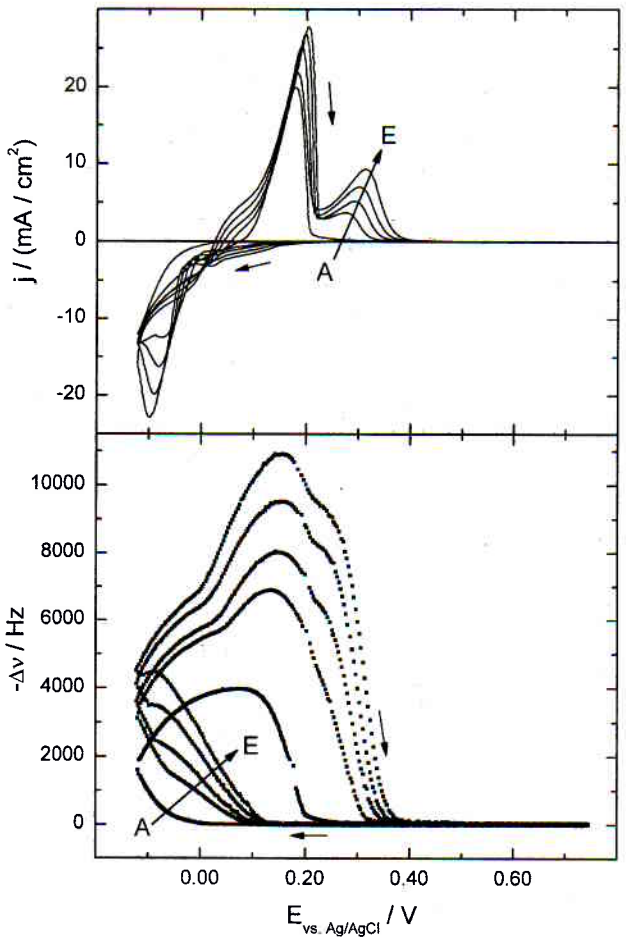

Fig. 7. Effect of Cl^--concentration on cyclic voltammograms and frequency evolution curves. The concentration of Cl^- increases from A to E (0, 9.84, 19.6, 30.2, 42.2 mmol/kg).

Fig. 8 shows the peak current density of the CuCl dissolution peaks with respect to the chloride concentration. A linear correlation of current density can be found, showing a slope of 172.8 ± 5.9 mA kg/C m² mol. The first anodic peak can clearly be

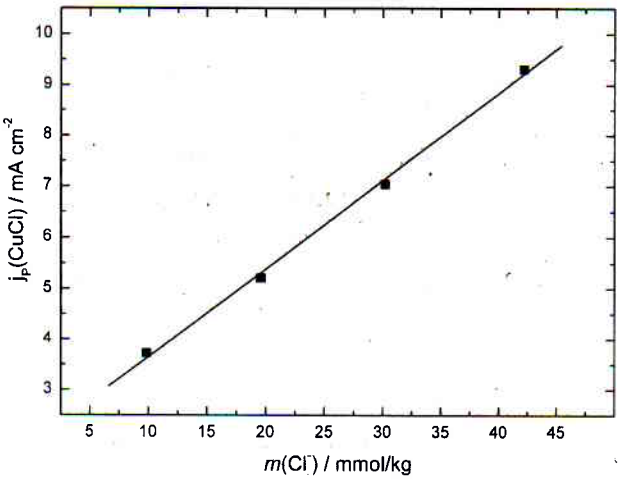

Fig. 8. Peak current density of the CuCl(s) dissolution at approx. 0.30 V with respect to the Cl^- concentration.

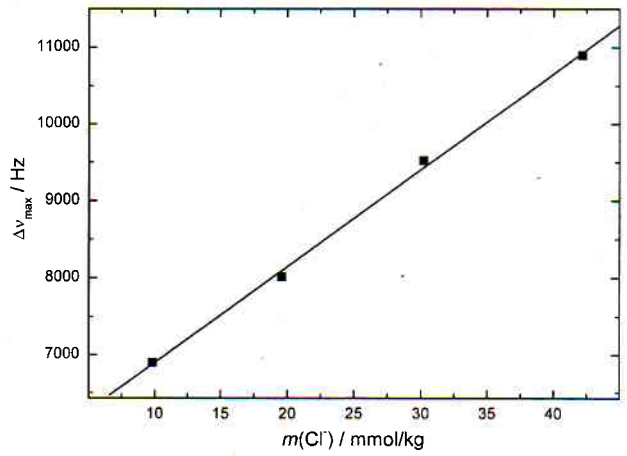

Fig. 9. Maximum frequency shift obtained during the CuCl(s) formation peak as a function of Cl^- concentration.

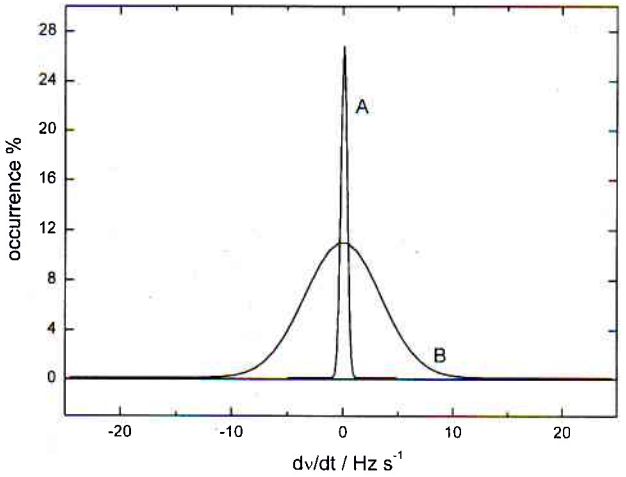

Fig. 11. Comparison of the noise behaviour of a 1.0 in. (A) and a 0.55 in. (B) diameter quartz crystal measured using the authors' fast impedance scanning QCM device, for details see text.

attributed to the formation of CuCl(s) on the electrode which is dissolved during the second anodic peak. Fig. 9 correlates the maximum frequency shift obtained during a CV-scan with the chloride concentration. A linear dependence with a slope of 125.3 ± 3.8 kHz kg/mol can be realized.

Fig. 10 shows a typical impedance scan and the curve fitted via Eq. (2). In this example, a statistical significance of about $\chi^2 = 1 \times 10^{-7}$was calculated. An optional non-linear fit according to Eq. (1), using the parameters from the linear fit was evaluated. It could be shown that χ^2 of both fitting types differs only by maximal 6%. A Gauß–Newton fit converges within two iteration steps to less than 0.01% of the relative deviation of χ^2. Comparing linear and non-linear fitting methods, the frequency deviations were found to be in the ppm-range and to be statistically distributed during the measurement procedure. The remarkable time advantage of the linear method outweighs these negligible errors.

In Fig. 11, the noise analysis of the resonance frequency is shown. For this a baseline was acquired over 1 h with the normally used 0.55 in. and, for comparison, a 1.0 in. diameter quartz crystal from Maxtek, part number 149240-1. The experiments were conducted in a cell containing purified water. The baseline was derived numerically and the occurrence of frequencies at distinct intervals of 0.2 Hz was counted. The Gaussian-type distributions were evaluated in respect to the 95% confidence interval. The 1.0 in. diameter crystal shows a deviation of 0.5 Hz from the mean value. The same experiment was conducted with the commercially available Maxtek RQCM device resulting in a deviation of 3.2 Hz. Using the very cost efficient, but in electrochemistry not commonly used, 0.55 in. diameter crystal the authors' QCM device was able to achieve 7 Hz. This is an acceptable value compared to 700 Hz of the Maxtek RQCM. The high damping of the small crystal inhibits a proper locking of the phase locked oscillator. This results in random frequency hopping and shows the technical superiority of the fast impedance scanning design.

Fig. 12 presents typical spectra for the polymerization of aniline recorded with our equipment during CV. Even after 25 cycles and a film thickness of approx. 1.0 μm, the strongly damped magnitude of the quartz crystal response can be reliably evaluated by the

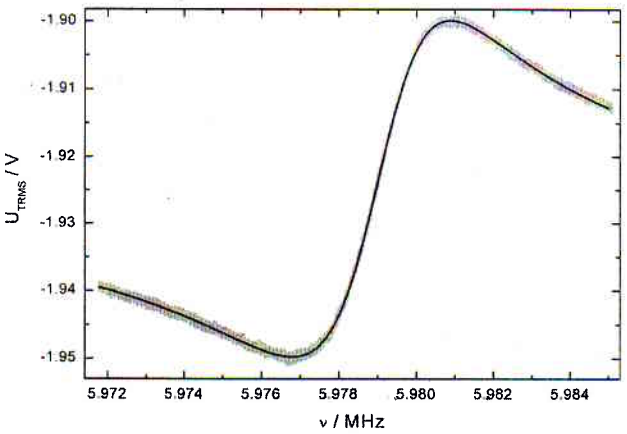

Fig. 10. Unprocessed response signal (U_{TRMS}) of the TRMS-converter as function of the frequency ν (scattered line). Data acquisition was performed within about 100 ms. A linear fit of 53,000 datapoints is treated within 44 ms. An optional non-linear fit converges within 107 ms over two iterations and shows no significant improvement. The two fitted curves (solid lines) cannot be distinguished in this graph.

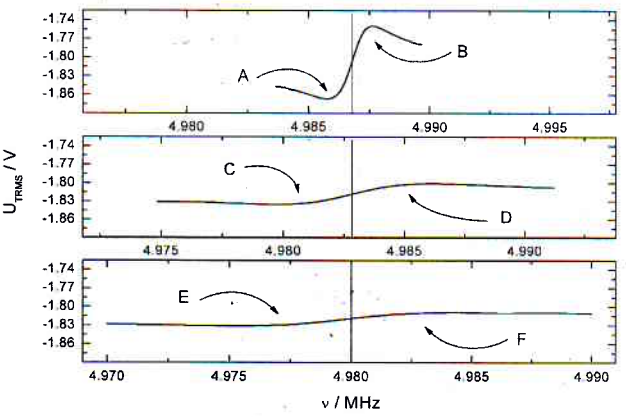

Fig. 12. Typical magnitude response of the quartz crystal under varying load. Electrodeposition of polyaniline was monitored by a cyclic voltammetry experiment. For details see text. The initial series and parallel resonace frequencies, A and B can be determined very exactly. After 21 cycles (C, D) and 25 cycles (E, F) these frequencies can still be reliably determined by the software algorithm. The spectra were conducted at a cathodic potential of approx. 0.61 V. The reduced quality factor $\hat{Q}$ decreases from 0.9996 over 0.9987 to 0.9982. Frequencies in MHz: $A = 4.98571$, $B = 4.98767$, $C = 4.97970$, $D = 4.98614$, $E = 4.97531$, $F = 4.98426$.

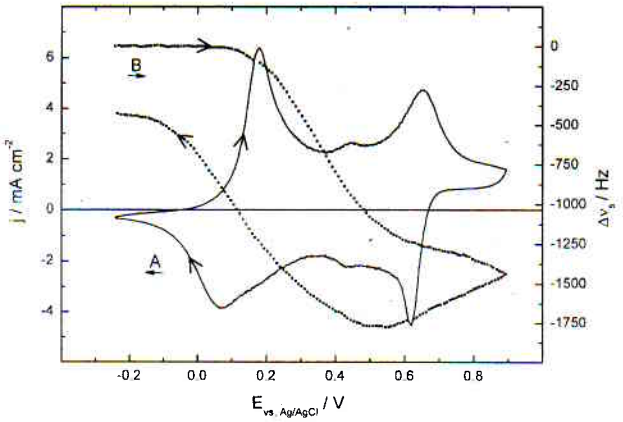

Fig. 13. Cyclic voltammogram (A) and frequencogram (B) of 0.1 mol/L aniline in 1 mol/L phosphoric acid. The 21st cycle is shown.

software algorithm; oscillation with the conventional Maxtek RQCM completely fails. The estimate of the film thickness was based on coulometric mechanistic estimations done by [27] and assuming a specific PANI density of 1.33 g/cm^3 [34].

Fig. 13 shows the cyclic voltammogram and the frequency evolution curve for the 21st cycle. At the potential of 0.18 V the radical cation of the aniline polymer is generated [27] at the first anodic peak by oxidation and is deposited with growing potential resulting in a second anodic peak at 0.65 V. Peak currents are observed to increase generally from cycle to cycle. The mass increase is monitored to start beginning with the first anodic peak, showing the polymerization's chain propagation [27]. The increase stops at about 0.5 V, the intersection of the cathodic peaks at 0.61 V and 0.42 V. Subsequently, the mass loading decreases, resulting in a mass and frequency hysteresis. Polyaniline is deposited irreversibly onto the quartz electrode.

4. Conclusions

With common electrochemical experiments we have shown that our new EQCM device works well. Many advantages as compared to other systems will make this design attractive for research and development tasks. The device is usable for strongly damped crystals in contact with liquids. Even the small and cheap 0.55 in. diameter crystals can be used instead of the very expensive 1.0 in. diameter quartzes. No manual compensation of parasitic capacities is needed which is common for oscillator designs. The exciting amplitude can be adjusted in a very comfortable manner. First studies have shown, that the hardware design is usable even for arrays of crystals with different fundamental frequencies in parallel connection option [35]. Monitoring impedance scans during the measurement enables detection of interferences that reduce the quality. Resonance frequencies in a range between 1 and 15 MHz are determined via a software algorithm so that changes in the function can easily be applied without the need to change the hardware itself. A cost-effective design using highly integrated devices and a very small overall dimension of 160 mm × 100 mm × 51 mm was reached. The electrical connection to the sensor crystal is completely DC decoupled enabling the combination with an electrochemical equipment in a very comfortable and stable manner. A graphical controlling software allows intuitive and user-friendly operation and the digital link to measurement data from the electrochemical equipment allows data transfer and correlations with very high accuracy, without detouring over analog inputs and outputs at separate devices. Scan rates faster than 500 kS/s allow fast and reliable data collection with a maximal frequency resolution down to 20 mHz. Applying a linear data fit algorithm instead of a non-linear model assures the stable evaluation of the generated data and a constant data-rate.

QCM and EQCM studies are very powerful methods in science and other applications, such as life-sciences. The impedance scanning approach in QCM instrumentation has been accepted to be superior to the oscillator approach especially for heavily damped crystals. Up to now it is considered to be not only highly priced but also far too slow for EQCM applications [13]. This is especially true with commercially available impedance analyzers for universal use. The authors' design overcomes these former disadvantages. By using only a few highly integrated circuits the hardware of the QCM is very cost-efficient. The determination of the resonance frequency is done automatically and rapidly on a common personal computer by use of a linear fit of a rational function, a Padé approximant. We feel that this approach should be able to extend the use of impedance scanning methods in (E)-QCM applications.

Acknowledgements

Thanks to Prof. Glenn Hefter (Murdoch University, Australia), Sandra Zugmann, and Dominik Moosbauer for editing, to our industrial partners (Infineon, Merck, Fortu, C3 Prozess- und Analysentechnik), and the DFG (SPP 1191—"Ionic Liquids" and "DFG-Projektinitiative: Funktionsmaterialien und Materialanalytik zu Lithium-Hochleistungsbatterien") for funding our work and to Dr. Edith Schnell (University of Regensburg) for AFM observations and interpretations.

References

[1] G. Sauerbrey, Z. Phys. A 155 (1959) 206.
[2] K. Doblhofer K.G., Bunsen Mag. 9 (2007) 162.
[3] D.A. Buttry, M.D. Ward, Chem. Rev. 92 (1992) 1355.
[4] R.P. Buck, E. Lindner, W. Kutner, G. Inzelt, Pure Appl. Chem. 76 (2004) 1139.
[5] F. Temurtas, C. Tasaltin, H. Temurtas, N. Yumusak, Z. Ozturk, in: A. Yazici, C. Sener (Eds.), Fuzzy Logic and Neural Network Applications on the Gas Sensor Data: Concentration Estimation, Springer Verlag, Berlin, Heidelberg, 2003, p. 179.
[6] E. Gileadi, V. Tsionsky, J. Electrochem. Soc. 147 (2000) 567.
[7] Z. Shen, M. Huang, C. Xiao, Y. Zhang, X. Zeng, P.G. Wang, Anal. Chem. 79 (2007) 2312.
[8] A. Sajula, D.S. Kalonia, AAPS Pharm. Sci. Tech. 5 (2004) 47.
[9] A.L. Kipling, M. Thompson, Anal. Chem. 62 (1990) 1514.
[10] A.F. Holloway, A. Nabok, M. Thompson, A.K. Ray, T. Wilkop, Sens. Actuators B 99 (2004) 355.
[11] R. Lucklum, P. Hauptmann, Anal. Bioanal. Chem. 384 (2006) 667.
[12] S.J. Martin, V.E. Granstaff, G.C. Frye, Anal. Chem. 63 (1991) 2272.
[13] F. Eichelbaum, R. Borngraeber, J. Schroder, R. Lucklum, P. Hauptmann, Rev. Sci. Instrum. 70 (1999) 2537.
[14] K.K. Kanazawa, Analyst 130 (2005) 1459.
[15] A. Arnau, Sensors 8 (2008) 370.
[16] P. Horowitz, W. Hill, Die Hohe Schule der Elektronik, 8th ed., Analogtechnik, Elektor Verlag, 2006.
[17] A. Krzywaznia, J. Ociepka, Meas. Sci. Technol. 11 (2000) N20.
[18] J. Schroder, R. Borngraeber, F. Eichelbaum, P. Hauptmann, Sens. Actuators A 97 (2002) 543.
[19] J. Auge, K. Dierks, F. Eichelbaum, P. Hauptmann, Sens. Actuators B 95 (2003) 32.
[20] J. Schroder, R. Borngraeber, R. Lucklum, P. Hauptmann, Rev. Sci. Instrum. 72 (2001) 2750.
[21] L.A. Delia, P. Vanysek, Electroanalysis 18 (2006) 371.
[22] J. Kankare, K. Loikas, M. Salomaki, Anal. Chem. 78 (2006) 1875.
[23] L. Bruschi, G. Delfitto, G. Mistura, Rev. Sci. Instrum. 70 (1999) 153.
[24] W.H. Press, S.A. Teukolsky, W.T. Vetterling, B.P. Flannery, Numerical Recipes in C, 2nd ed., Press Syndicate of the University of Cambridge, 1992.
[25] V.M. Krasnopolsky, V.I. Kukulin, J. Horácek, Czech. J. Phys. 39 (1989) 593.
[26] J. Barthel, R. Neueder, Chemical Thermodynamics, Academic Press, New York, 2001, p. 767.
[27] H. Eisazadeh, K.J. Gilmore, A.J. Hodgson, G. Spinks, G.G. Wallace, Colloids Surf. A 103 (1995) 281.
[28] Q. Xie, Z. Li, C. Deng, M. Liu, Y. Zhang, M. Ma, S. Xia, X. Xiao, D. Yin, S. Yao, J. Chem. Educ. 84 (2007) 681.

[29] G. Vatankhah, J. Lessard, G. Jerkiewicz, A. Zolfaghari, B.E. Conway, Electrochim. Acta 48 (2003) 1613.
[30] S. Ye, C. Ishibashi, K. Shimazu, K. Uosaki, J. Electrochem. Soc. 145 (1998) 1614.
[31] S. Kologo, M. Eyraud, L. Bonou, F. Vacandio, Y. Massiani, Electrochim. Acta 52 (2007) 3105.
[32] D. Giménez-Romero, C. Gabrielli, J.J. Garcá-Jareño, H. Perrot, F. Vicente, J. Electrochem. Soc. 153 (2006) J32.
[33] K. Doblhofer, S. Wasle, D.M. Soares, K.G. Weil, G. Ertl, J. Electrochem. Soc. 150 (2003) C657.
[34] J. Stejskal, I. Sapurina, J. Prokes, J. Zemek, Synth. Met. 105 (1999) 195.
[35] S. Guan, R.B. Nielsen, Rev. Sci. Instrum. 74 (2003) 5241.